PROCEEDINGS B

royalsocietypublishing.org/journal/rspb

Research

Cite this article: Griem-Krey H, Petersen C, Hamerich IK, Schulenburg H. 2023 The intricate triangular interaction between protective microbe, pathogen and host determines fitness of the metaorganism. *Proc. R. Soc. B* **290**: 20232193.
https://doi.org/10.1098/rspb.2023.2193

Received: 26 September 2023
Accepted: 7 November 2023

Subject Category:
Evolution

Subject Areas:
evolution, ecology

Keywords:
metaorganism, *Caenorhabditis elegans*, host–microbiota interactions, protective bacteria, *Pseudomonas lurida*, *Bacillus thuringiensis*

Author for correspondence:
Hinrich Schulenburg
e-mail: hschulenburg@zoologie.uni-kiel.de

†Shared first authorship.

Electronic supplementary material is available online at https://doi.org/10.6084/m9.figshare.c.6935806.

THE ROYAL SOCIETY PUBLISHING

The intricate triangular interaction between protective microbe, pathogen and host determines fitness of the metaorganism

Hanne Griem-Krey[1,†], Carola Petersen[1,†], Inga K. Hamerich[1] and Hinrich Schulenburg[1,2]

[1]Department of Evolutionary Ecology and Genetics, Kiel University, Kiel 24118, Germany
[2]Antibiotic resistance group, Max-Planck-Institute for Evolutionary Biology, Plön, Germany

CP, 0000-0002-2164-6789; IKH, 0000-0002-3451-4574; HS, 0000-0002-1413-913X

The microbiota shapes host biology in numerous ways. One example is protection against pathogens, which is likely critical for host fitness in consideration of the ubiquity of pathogens. The host itself can affect abundance of microbiota or pathogens, which has usually been characterized in separate studies. To date, however, it is unclear how the host influences the interaction with both simultaneously and how this triangular interaction determines fitness of the host–microbe assemblage, the so-called metaorganism. To address this current knowledge gap, we focused on a triangular model interaction, consisting of the nematode *Caenorhabditis elegans*, its protective symbiont *Pseudomonas lurida* MYb11 and its pathogen *Bacillus thuringiensis* Bt679. We combined the two microbes with *C. elegans* mutants with altered immunity and/or microbial colonization, and found that (i) under pathogen stress, immunocompetence has a larger influence on metaorganism fitness than colonization with the protective microbe; (ii) in almost all cases, MYb11 still improves fitness; and (iii) disruption of p38 MAPK signalling, which contributes centrally to immunity against Bt679, completely reverses the protective effect of MYb11, which further reduces nematode survival and fitness upon infection with Bt679. Our study highlights the complex interplay between host, protective microbe and pathogen in shaping metaorganism biology.

1. Introduction

The association between a host and its microbiota is central to the biology and fitness of the host and can influence its development, physiology, immunity, reproduction, stress resistance and even behaviour [1–3]. Hosts and associated microbes are thus often considered to form a metaorganism, which can include all kinds of microorganisms, ranging from mutualists over commensals to pathogens, and where the involved members influence each other's fitness [4,5]. Genetic and resulting phenotypic variation in the metaorganism can result from both changes in the host genome and changes in the microbiota, the latter including the acquisition of new microbes or alterations of relative species abundance [2,6,7]. As a consequence, the microbiota may influence the distribution of host phenotypes within a population and thus shape the evolutionary trajectory of the host [6,8].

One important evolutionary advantage the microbiota provides to its host is protection against invading pathogens [9]. Microbiota-mediated protection can occur through several mechanisms, including direct interaction with the pathogen through secretion of antimicrobial products or resource competition [10–13], or indirectly through induction of the host's immune system [14–16]. Changes in the microbiota may therefore alter host susceptibility to infections [17,18]. Moreover, the microbiota not only contains beneficial but also potentially

harmful microbes. For example, *Candida albicans* is commonly found in the gut of humans but overgrowth due to changes in host immunity or microbiota causes opportunistic infections [19,20]. Additionally, pathogens have evolved mechanisms to promote their growth despite the microbiota or even use the microbiota to facilitate infection [21–24]. Invading pathogens may trigger changes in the microbiota causing otherwise neutral or beneficial microbes to become harmful [25,26]. Hence, beneficial and harmful microbes can interact with each other, and this interaction has consequences for the host, thereby shaping the phenotype and fitness of the metaorganism as a whole.

The host, and particularly the host immune system, directly affects both beneficial and pathogenic microorganisms. The importance of the immune system in controlling and eliminating pathogenic microbes is very well researched and forms the main basis of our current understanding of animal immunity. The host's immune system also plays a central role in shaping the composition of its microbiome, as demonstrated for a diversity of host systems, ranging from early branching metazoans, such as *Hydra* polyps [27], to flies and worms [28–31], bobtail squids [32] and vertebrates and humans [33,34]. To date, it is unclear how exactly the host immune system simultaneously influences the abundance of both the protective microbe and the pathogen, and thereby shapes metaorganism biology [35,36]. Additional host factors may similarly and simultaneously affect the presence of both beneficial microbes and pathogens, for example host traits influencing uptake dynamics in case of gut microbes. A more detailed analysis of the triangular interaction between host, beneficial microbe and pathogen is thus critical for our understanding of the biology and fitness of host organisms, as well as of the metaorganism as a whole, especially considering that pathogens are ubiquitous and that more or less all complex organisms are host to a diverse microbiota. One of the few exceptions that addressed this triangular interaction used a laboratory-based model, consisting of the nematode host *Caenorhabditis elegans*, the protective microbe *Enterococcus faecalis* and the pathogenic bacterium *Staphylococcus aureus* [37]. Although the two microbes are unlikely to coexist with *C. elegans* in nature, their experimental analysis yielded important insights into the principles that shape the evolution of symbiosis. Of relevance here is the finding that the host can evolve to harbour a larger number of the protective bacteria, thereby exploiting the function provided by the symbiont [38]. This effect appears to be mediated (at least to some extent) by the host immune system, for example by the lysozyme gene *lys-7*, which was identified to be part of the symbiont-dependent protective effect and which directly reduces pathogen-mediated killing and, at the same time, favours abundance of the protective symbiont over the pathogen [39]. It is currently unknown whether this host immunity-mediated effect translates into a competitive fitness advantage.

The aim of the current study is to assess the consequences of specific host traits for the interaction with both protective microbes and pathogens and ultimately metaorganism fitness. To address this aim, we focused on a model triangular interaction that included *C. elegans* as a host and its naturally associated protective symbiont, *Pseudomonas lurida* MYb11, as well as its pathogen *Bacillus thuringiensis*. Over the past two decades, the nematode has been used intensively for studying invertebrate immunity, with detailed information available on defence against *B. thuringiensis*, which includes insulin-like and p38 mitogen-activated protein kinase (MAPK) signalling [40–43], but not transforming growth factor beta (TGF-β) signalling that is involved in immunity against other pathogens [44]. More recent research efforts have been directed to the study of *C. elegans*–microbiota interactions [45–47]. In nature, the nematode is associated with a species-rich microbiota [48,49], which includes protective microbes, such as a variety of *Pseudomonas* species, that assist the host in its defence against pathogens [50,51]. Moreover, innate immunity [28,29,52] and microbe–microbe interactions have been shown to influence *C. elegans* microbiota composition and function [49,53]. For the current study, we used different *C. elegans* mutants, which allowed us to manipulate key traits affecting host immunity (e.g. p38 MAPK and TGF-β signalling) or microbial colonization of the host, for example through disruption of the grinder in the nematode's pharynx. The *C. elegans* mutants and wild-type were exposed in different combinations to the protective symbiont *P. lurida* MYb11 and pathogenic *B. thuringiensis* MYBT18679 (Bt679), followed by assessment of microbial colonization rates, nematode survival, nematode population growth, and importantly, nematode competitive fitness. MYb11 was previously shown to produce an antimicrobial compound, massetolide E, that directly inhibits Bt679, thereby increasing survival of infected *C. elegans* [50]. Based on the available information, we expected that an intact host immune response and/or a high colonization rate with the protective MYb11 should increase metaorganism fitness.

2. Material and methods

(a) Nematode and bacterial strains

The *C. elegans* strains used in this study are listed in table 1. Prior to all experiments, *C. elegans* strains were thawed from frozen stocks, maintained on nematode growth medium (NGM) on *Escherichia coli* strain OP50, and synchronized by bleaching following standard procedures [54].

Pseudomonas lurida MYb11 was used as a representative, protective natural microbiota member of *C. elegans* [48,50]. *Bacillus thuringiensis* MYBT18679 (Bt679), which produces pore-forming toxins, was used as a pathogen. The standard laboratory food bacterium *E. coli* OP50 and the non-pathogenic *B. thuringiensis* strain 407 Cry- (Bt407) were used as control bacteria. For each experiment, MYb11 and OP50 were freshly thawed from frozen stocks and grown on tryptic soy agar (TSA) plates at 25°C for 2 days. Liquid cultures were produced from single colonies grown in tryptic soy broth in a shaking incubator overnight at 28°C and adjusted to $OD_{600}10$ in phosphate-buffered saline (PBS). *B. thuringiensis* spore stocks were prepared as previously described and frozen in aliquots at −20°C [43,50,55]. Aliquots with spore concentrations ranging from 10^9–10^{10} particles/ml for Bt679 and 10^3–10^4 particles/ml for Bt407 were freshly thawed for each experiment. All experiments were performed on peptone-free nematode growth medium (PFM) to avoid germination of *B. thuringiensis* spores.

(b) Bacterial colonization assay

We assessed intestinal colonization by MYb11 following the previously described protocol [51,56,57]. Briefly, *C. elegans* were grown until the 4th instar larval (L4) stage on PFM plates inoculated with MYb11 or OP50. L4 were transferred to 60 mm PFM plates inoculated with 500 µl MYb11 or OP50 with or without

Table 1. *Caenorhabditis elegans* wild-type, nine mutant strains and one transgenic strain used in this study. GFP, green fluorescent protein.

strain[a]	genotype	description
N2	wild-type	wild-type
dbl-1	*dbl-1(nk3)*	TGF-β defective
sma-6	*sma-6(e1482)*	TGF-β defective
phm-2	*phm-2(ad597)*	grinder defective
tnt-3	*tnt-3(ok1011)*	grinder defective
daf-2	*daf-2(e1370)*	insulin-like signalling defective
daf-16	*daf-16(mgDf50)*	insulin-like signalling defective
tir-1	*tir-1(tm3036)*	p38 MAPK defective
pmk-1	*pmk-1(km25)*	p38 MAPK defective
nhr-8	*nhr-8(ok186)*	nuclear hormone receptor defective
CL2122	*dvIs15 [(pPD30.38) unc-54(vector) + (pCL26) mtl-2::GFP]*	GFP-labelled reference strain

[a]Strain names used throughout the manuscript.

B. thuringiensis Bt679 (1 : 200 if not stated otherwise). After 24 h at 20°C, adult worms were washed off the plates using 1.5 ml M9-buffer with 0.025% Triton-X 100 (M9-T). After washing five times with 1 ml M9-T, 100 µl worm pellet was transferred to a new microtube and 100 µl 10 mM tetramisole hydrochloride were added to stop pharyngeal pumping and excretion of bacteria. Worms were surface sterilized using M9-T with 2% sodium hypochlorite and washed twice in 1 ml PBS with 0.025% Triton-X 100 (PBS-T). Next, approximately 30 worms were transferred to a new sterile 2 ml microtube. The exact worm number was recorded for calculation of the colonization rate per worm. The volume of the transferred worms was topped up to 400 µl with PBS-T and 10–15 1 mm zirconia beads were added. In total, 100 µl supernatant were transferred to a new sterile microtube, of which 50 µl were plated onto TSA as a control for the surface sterilization process. Worms were shredded in the remaining 300 µl PBS-T using a Bead Ruptor 96 (OMNI International, Kennesaw, GA, USA) for 3 min at 30 Hz. 50 µl of serially diluted, homogenized worms in PBS-T (10^{-1} to 10^{-3}) were plated onto TSA. After approximately 24 h at 25°C, colonies were counted. For Bt679-infected worms, colonies of MYb11 or OP50 and Bt679 were morphologically distinguished and counted on the same plate. For all bacteria, colony forming units (CFU) per worm were calculated.

(c) *Bacillus thuringiensis* survival assay

Bacillus thuringiensis survival assays were performed as previously described [43,50,51] to characterize microbiota-mediated protection against Bt679 in the different *C. elegans* mutants. Briefly, L4 larvae grown on MYb11 or OP50 on PFM plates were washed five times in sterile M9-buffer. Approximately 30 washed L4 larvae were transferred to 60 mm PFM plates inoculated with 75 µl of Bt679 spore solution mixed 1 : 25, 1 : 50, 1 : 100, 1 : 200 or 1 : 500 with MYb11 or OP50. Plates inoculated with the non-pathogenic Bt407 mixed with MYb11 or OP50 at the highest concentration used for pathogenic Bt679 served as controls. After 24 h at 20°C, the number of dead and alive worms was counted. Worms were considered dead if they failed to respond to light touch. The survival rate was determined as proportion of worms alive.

(d) Population growth rate

As a proxy for fitness of the *C. elegans* strains when challenged with Bt679, a population growth assay was performed as previously described [48,50,51,58]. Briefly, *C. elegans* were grown on MYb11 or OP50 on PFM plates until L4 stage. Three L4 larvae were picked onto 90 mm PFM plates inoculated with 1 ml Bt679 or Bt407 spore solution mixed 1 : 200 with MYb11 or OP50 (worms were maintained on the same non-pathogenic bacteria as during larval development). After 5 days at 20°C, the worms were washed off the plates using 5 ml M9-T and directly frozen at −20°C until scoring. Worms on plates with low worm counts were scored directly. For scoring, frozen samples were thawed, mixed thoroughly, and the worms counted in triplicates in droplets ranging from 10 to 100 µl depending on worm density, followed by calculation of the offspring number per worm.

(e) Competitive fitness assay

We assessed the effect of the different microbiota-mediated effects on competitive fitness of the *C. elegans* mutants. Competitive fitness was determined using a population growth assay where the considered *C. elegans* mutants were always competed against a reference *C. elegans* strain, the transgenic strain CL2122, which produces a strong constitutive intestinal expression of GFP at all developmental stages [59]. To control for potential effects of GFP labelling, competition between CL2122 and wild-type N2 was additionally tested. Three *C. elegans* CL2122 and three mutant L4 worms were picked to PFM plates inoculated with MYb11 or OP50 with or without Bt679 (1 : 500). The competition experiment was performed either on 60 mm PFM plates on 500 µl of Bt679 mixture or, because of high progeny numbers, on 90 mm PFM plates on 1 ml of MYb11 or OP50 in the absence of Bt679. The worms were washed off the plates with or without Bt679 after 5 or 4 days, respectively. The numbers of fluorescent and non-fluorescent worms were counted in triplicates in droplets of 5–20 µl depending on worm density using a fluorescent dissecting scope (Leica Microsystems GmbH, Wetzlar, Germany). Competitive fitness was determined as the relative proportion of non-fluorescent mutant worms compared to the fluorescent reference strain CL2122.

(f) Statistical analysis

Statistical analyses and figures were done using R (v. 4.1.2) [60]. Graphs were plotted using the package ggplot2 [61] and edited in Inkscape (v. 1.1.2; see https://inkscape.org). The raw data can be found in electronic supplementary material, table S1. The results of the statistical tests performed on the phenotypic raw data can be found in electronic supplementary material, table S2. Parametric tests were used if the data met the assumptions, otherwise equivalent non-parametric tests were used. Assumptions of normality of data were confirmed with the Shapiro–Wilk test and equality of variances with *F*-tests [62,63]. A binomial generalized linear model was used to compare differences in survival [64], followed by Tukey's test [65]. Wilcoxon rank-sum tests were applied to assess differences in bacterial load and population growth [66]. One sample *t*-tests were used to evaluate differences between *C. elegans* strain proportions after competition to the theoretical value of 0.5, while two sample *t*-tests served to assess variation in competitive fitness on OP50 and MYb11 [67]. False discovery rate (FDR) correction was used to account for multiple testing where appropriate [68]. Observer bias was minimized by coding of samples and the compared treatments were assayed in parallel in randomized

arrangements. In the initial analysis of the nine *C. elegans* mutants, one replicate was excluded from the data because it clearly displayed an experimental error (absence of worms).

3. Results

(a) Interactions between diverse host genes and the protective *P. lurida* MYb11 shape *C. elegans* pathogen resistance

As a first step of our study, we explored variation among all considered *C. elegans* mutants in two traits: colonization by the protective *P. lurida* MYb11 and survival upon Bt679 infection. The results of this survey were then used to choose a subset of mutants for further analysis. The considered mutants either showed impaired immunity or altered microbial uptake, which potentially influences microbiota abundance [28,29,52,69]. We found that MYb11 colonization was significantly higher in the mutants *dbl-1*, *sma-6*, *phm-2*, *tnt-3* and *tir-1* compared to the wild-type N2 ($p < 0.05$). By contrast, *daf-2* mutants showed lower MYb11 colonization ($p = 0.022$), while the mutants *pmk-1*, *daf-16 and nhr-8* did not differ from N2 (electronic supplementary material, figure S1*a* and table S2). We further found that survival upon Bt679 infection was significantly lower in the MYb11-fed *phm-2*, *tnt-3*, *tir-1* and *pmk-1* mutants compared to N2 ($p < 0.001$), while there was no difference in survival between the mutants *dbl-1*, *sma-6*, *daf-2*, *nhr-8* and N2 (electronic supplementary material, figure S1*b* and table S2). Based on these results, we selected four strains with contrasting patterns for a more in-depth characterization, including the mutants *dbl-1* (high colonization, high survival), *phm-2* (high colonization, low survival), *pmk-1* (low colonization, low survival) and the wild-type strain N2 (low colonization, high survival).

(b) Infection with *B. thuringiensis* alters intestinal colonization rates in *C. elegans*

In a bacterial colonization assay (figure 1*a*), we subsequently tested whether Bt679 infection alters the intestinal colonization rate with MYb11 or *E. coli* OP50. On Bt679, *dbl-1* mutants showed decreased MYb11 colonization ($p = 0.039$) and colonization with OP50 was decreased in *phm-2* mutants ($p = 0.039$) (figure 1*b*; electronic supplementary material, table S2). For *pmk-1* mutants an opposite trend was observed, namely that MYb11 colonization was increased on Bt679 ($p = 0.057$). Except for the *pmk-1* mutant, MYb11 colonization was higher than OP50 colonization in all worm strains ($p < 0.05$). For the *pmk-1* mutant, a trend towards higher MYb11 colonization compared to OP50 colonization was observed without Bt679 ($p = 0.057$). Albeit not statistically significant, Bt679 was found in low numbers but more in *dbl-1* and *phm-2* mutants fed with MYb11 (figure 1*c*; electronic supplementary material, table S2).

(c) Disruption of p38 MAPK pathway and grinder abrogates the protective phenotype conferred by *P. lurida* MYb11

To assess the relative contributions of host and protective microbiota to pathogen resistance, we repeated the survival assay including worms grown on OP50. After Bt679 infection, survival of *C. elegans* N2 and the *dbl-1* mutant was higher on MYb11 than on OP50 ($p < 0.001$), with higher survival rates of *dbl-1* mutants compared to N2 on OP50 ($p < 0.001$) and MYb11 ($p = 0.016$) (figure 2; electronic supplementary material, table S2). *phm-2* mutants showed no difference in survival on MYb11 and OP50, but an overall higher survival than N2 on OP50 ($p = 0.009$). Survival of *pmk-1* mutants was generally lower than that of N2 ($p < 0.001$), with survival rates on MYb11 being significantly lower than those on OP50 ($p < 0.001$).

(d) Interactions between host, protective microbe and pathogen determine *C. elegans* population growth and competitive fitness

We subsequently measured nematode population growth in the presence or absence of Bt679 to determine the combined influence of host, protective microbiota and pathogen as a proxy for metaorganism fitness. All *C. elegans* strains showed decreased population growth on Bt679 compared to non-pathogenic Bt407 ($p < 0.01$) (figure 3; electronic supplementary material, table S2). Except for *pmk-1* mutants on Bt679, population growth rates were higher on MYb11 than OP50 ($p < 0.01$). On Bt679, the population growth rate of the *pmk-1* mutant was lower than that of N2 on MYb11 and OP50 ($p < 0.01$). The mutant strains *dbl-1* and *phm-2* always produced lower offspring numbers than N2 on both Bt679 and Bt407 ($p < 0.05$).

We further tested the competitive fitness of the mutant strains compared to the GFP-labelled reference strain CL2122 in population growth assays (figure 4*a*). The competitive fitness of *C. elegans* CL2122 and N2 did not differ, indicating that the GFP-label does not affect worm fitness (electronic supplementary material, tables S1 and S2). The proportions of the *dbl-1* mutant also showed no difference from the reference strain (figure 4*b*). *phm-2* mutants on MYb11 and OP50 without Bt679 showed lower competitive fitness compared to the reference strain ($p < 0.01$), and a trend towards lower fitness on OP50 with Bt679 ($p = 0.082$). Except for *pmk-1* mutants, competitive fitness of *C. elegans* on MYb11 and OP50 did not differ. Competitive fitness of *pmk-1* mutants was reduced compared to the reference strain for worms grown on OP50 ($p = 0.019$) and MYb11 ($p = 0.002$) with Bt679, with MYb11 resulting in even lower fitness than OP50 ($p = 0.019$). Conversely, when Bt679 was absent, then *pmk-1* mutants showed increased competitive fitness on MYb11 compared to on OP50 ($p = 0.001$), and on MYb11, the *pmk-1* mutant produced more offspring than the reference strain ($p < 0.001$).

4. Discussion

Our study assessed the triangular interaction between specific host traits, protective microbe and pathogen, and their influence on metaorganism fitness. We focused on *C. elegans* mutants with changes in two relevant traits, immunity and colonization by microbes, because each of these traits should simultaneously affect the interaction with both the protective microbe and the pathogen. We then asked how the affected *C. elegans* traits interact with the protective microbiota member *P. lurida* MYb11 to determine resistance, population growth and competitive fitness upon infection with the pathogen *B. thuringiensis* Bt679, thus considering two measures of

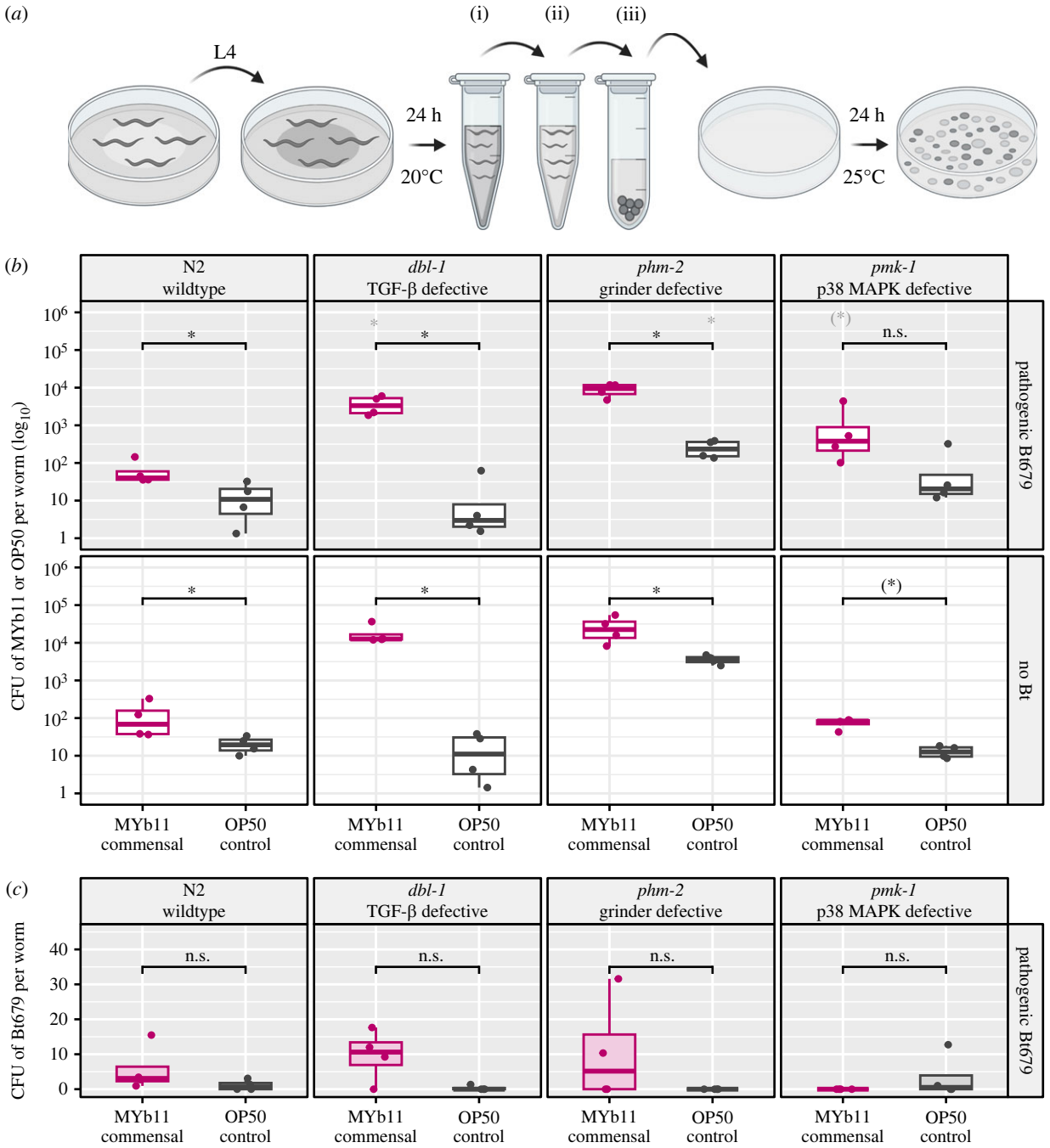

Figure 1. Intestinal colonization of *C. elegans* is influenced by host genotype and *B. thuringiensis* Bt679 infection. (*a*) Synchronized *C. elegans* were grown on *P. lurida* MYb11 or *E. coli* OP50 until the L4 stage. L4 worms were transferred to the same bacteria with or without the addition of Bt679 spores (1 : 200). A lower Bt concentration of 1 : 2000 was used for the *pmk-1* mutant to account for its high susceptibility to Bt679 infection. After 24 h, adult *C. elegans* were washed (i), surface sterilized (ii) and broken up (iii) to release the intestinal bacteria, which were plated out to count the colony forming units (CFU). (*b*) CFU of MYb11 (pink) or OP50 (grey) per worm with Bt679 (grey panel background) or without Bt679 (white panel background). For each *C. elegans* strain, asterisks denote significant differences between corresponding treatments with MYb11 or OP50 (black) or between corresponding treatments with and without Bt679 (grey). Note that the *y*-axis is $\log_{10}$-transformed. (*c*) CFU of Bt679 per worm on MYb11 (pink) or OP50 (grey). In (*b,c*) boxplots are shown with the median as a thick horizontal line, the interquartile range as box and the whiskers as vertical lines, and each replicate is depicted by a dot. Wilcoxon rank-sum test, corrected for multiple comparisons with FDR, $^{(*)}p < 0.1$, $^{*}p < 0.05$, $n = 4$. n.s., not significant.

nematode fitness (population growth and competitive fitness), taking advantage of the short generation time of *C. elegans*. The used *C. elegans* mutants are known to affect immunity and/or microbial colonization in distinct ways, including strains with high colonization and high pathogen survival (*dbl-1*), high colonization and low survival (*phm-2*), low colonization and low survival (*pmk-1*), and also low colonization and high survival in the wild-type N2. Our main findings (figure 5) are that (i) under pathogen stress, the immunocompetent wild-type N2 generally produces the highest competitive fitness and the highest population growth rate if compared to the mutant strains, suggesting that immunocompetence is more important than high colonization rates with the protective microbe (as documented for the *dbl-1* and *phm-2* mutants); (ii) association with the protective microbe *P. lurida* MYb11 rather than the standard laboratory food *E. coli* OP50 generally increases host performance under both pathogen and control conditions, suggesting a

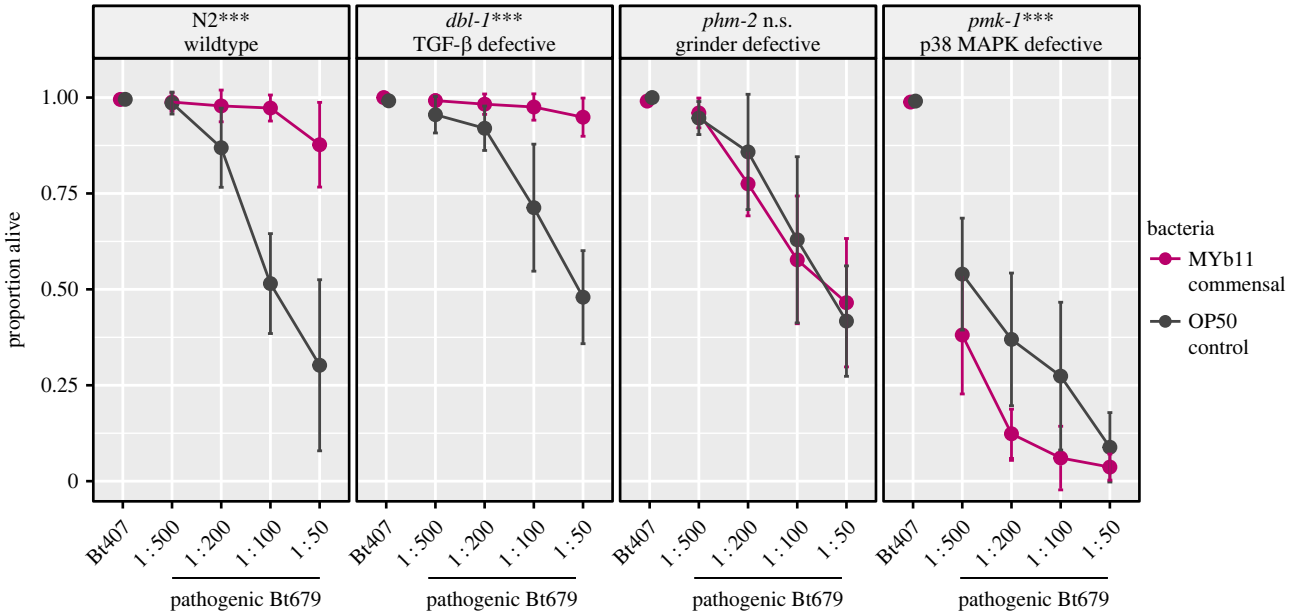

Figure 2. *Pseudomonas lurida* MYb11 protects *C. elegans* strains N2 and *dbl-1* against infection with Bt679, increases susceptibility of *pmk-1* and has no effect on survival of *phm-2*. Proportion of alive *C. elegans* N2 and *dbl-1*, *phm-2*, *pmk-1* mutants fed with MYb11 (pink) or *E. coli* OP50 (grey) 24 h after Bt679 infection. Non-pathogenic Bt407 (1 : 50) was used as control. Shown are the means as dots and the standard deviations as error bars, with each line representing the proportion of alive worms (survival) on different concentrations of Bt spores. Asterisks denote significant differences between worms on MYb11 and OP50. Generalized linear model, corrected for multiple comparisons with FDR, ***$p < 0.001$, $n = 8$.

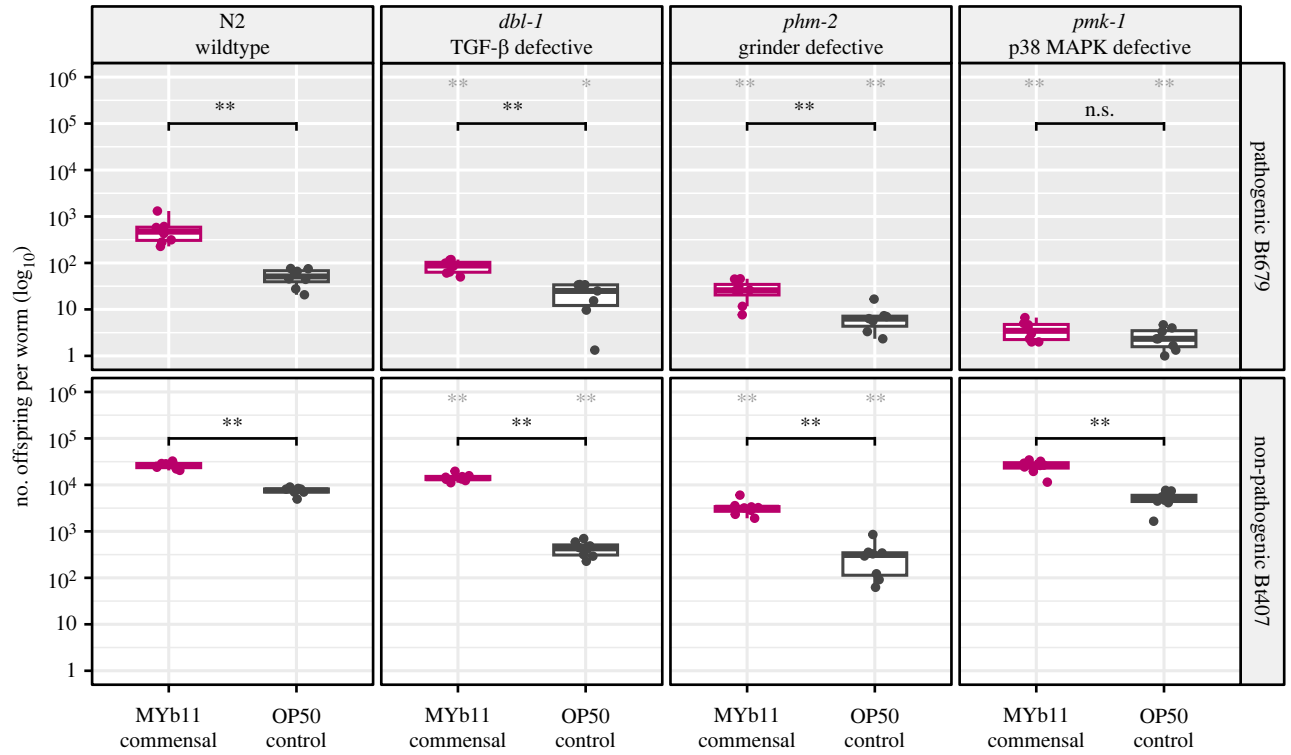

Figure 3. Population growth of *C. elegans* is influenced by host genotype, microbiota and pathogen. The population growth rate of the wild-type N2 and the mutants *dbl-1*, *phm-2*, *pmk-1* grown on either *P. lurida* MYb11 (pink) or *E. coli* OP50 (grey) was analysed on pathogenic Bt679 (grey panel background) and non-pathogenic Bt407 (white panel background) and is shown as number of offspring per initial worm. Shown are boxplots with the median as a thick horizontal line, the interquartile range as box, the whiskers as vertical lines and each replicate depicted by a dot. Asterisks denote significant differences between worms on MYb11 and OP50 (black) or between *C. elegans* mutant strains and wild-type N2 (grey). Wilcoxon rank-sum test, corrected for multiple comparisons with FDR, *$p < 0.05$, **$p < 0.01$, $n = 8$.

significant nutritional and/or protective impact of MYb11 on the host; and (iii) disruption of a Bt679-relevant component of the host immune system, the p38 MAPK signalling pathway, completely reverses the effect of the protective microbe, which under pathogen conditions further reduces nematode survival and competitive fitness, thus turning a beneficial interaction into a harmful interaction. In the following, we discuss how the results for each considered mutant enhances our understanding of the worm's interaction with protective symbionts and pathogens.

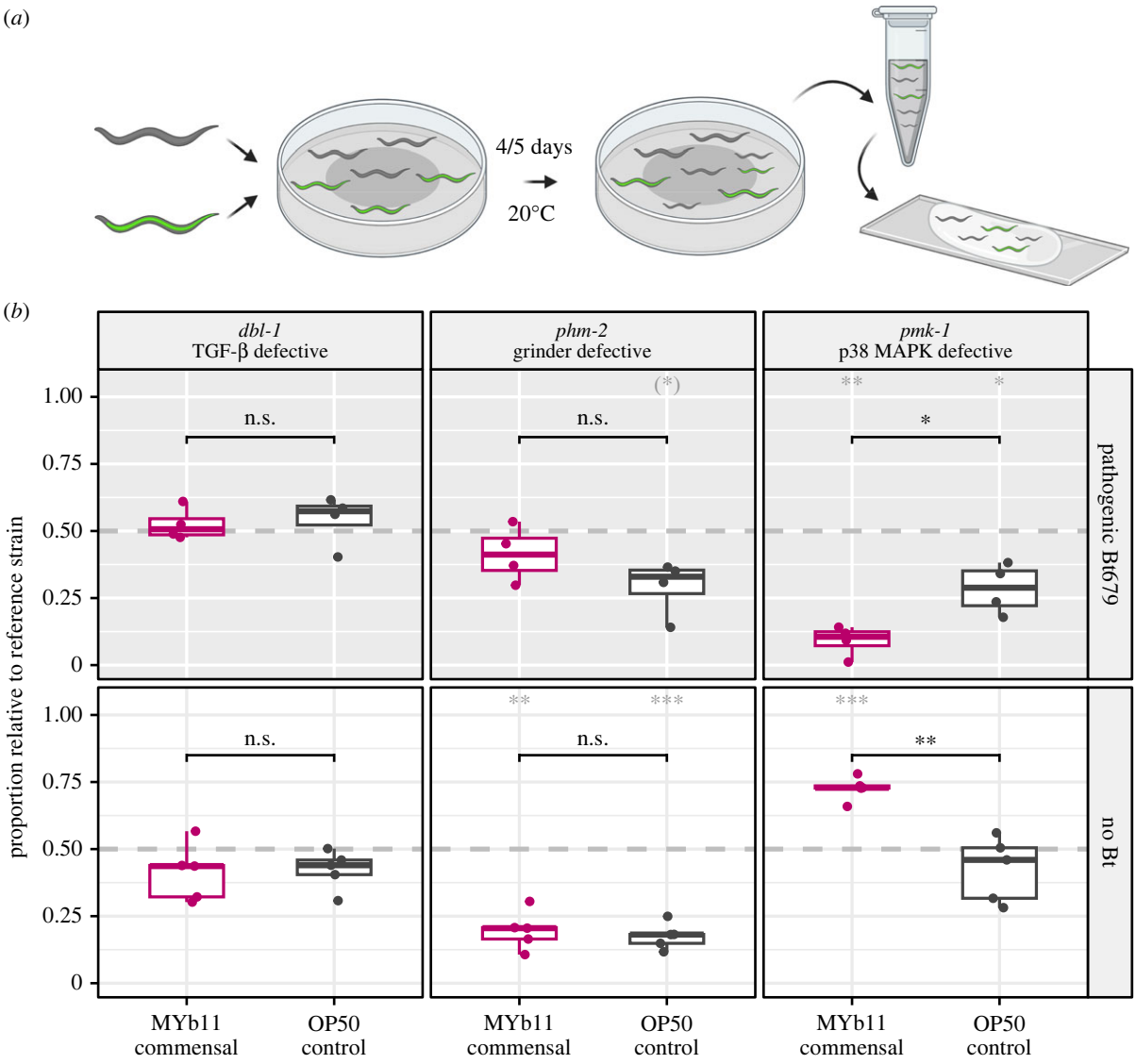

Figure 4. Competitive fitness of *C. elegans* is influenced by host genotype, protective microbe and pathogen. (*a*) Three L4 each of the GFP-labelled reference strain CL2122 and a mutant strain were placed on *P. lurida* MYb11 or *E. coli* OP50 with or without Bt679. After 4 (without Bt679) or 5 days (with Bt679), the relative proportion of mutant worms to the reference strain was determined. (*b*) Proportion of the *C. elegans* mutants *dbl-1*, *phm-2* and *pmk-1* relative to CL2122 on MYb11 (pink) or OP50 (grey) either with Bt679 ($n = 4$, with three technical replicates each, grey panel background) or without Bt679 ($n = 5$, with three technical replicates each, white panel background). Data are presented as boxplots with the median as a thick horizontal line, the interquartile range as box, the whiskers as vertical lines, and each replicate depicted by a dot. Grey asterisks denote significant differences between the proportion of the respective mutant strain and 0.5 (which is the expected proportion if mutant and wild-type are present in equal numbers), as inferred from one-sample *t*-tests, corrected for multiple comparisons with FDR. Black asterisks denote the difference between worms fed with MYb11 or OP50, as assessed with two sample *t*-tests, corrected for multiple comparisons with FDR. In both cases, $^{(*)}p < 0.1$, $^{*}p < 0.05$, $^{**}p < 0.01$, $^{***}p < 0.001$, n.s., not significant.

The *dbl-1* gene encodes one of four TGF-β ligands in *C. elegans* and it is central for the nematode TGF-β signalling cascade, which is involved in immune defence against fungi and some pathogenic Proteobacteria [70,71]. To date, this pathway was not previously known to contribute to defence against *B. thuringiensis*. Thus, our observation of an increased survival of the *dbl-1* defective mutant on Bt679, without MYb11 and relative to wild-type N2 (figure 2) suggests a previously unknown role of this pathway in immunity that appears to rely on its inactivation. Moreover, disruption of this pathway causes increased colonization by MYb11 (irrespective of pathogen environment; figure 1*b*). This result indicates that intact TGF-β signalling controls microbiota abundance, as previously reported for other microbiota members in *C. elegans*, including those from the families *Enterobacteriaceae* and *Pseudomonadaceae* [29]. The colonization with MYb11 then leads to increases in survival in the presence of the pathogen (figure 2) and population growth (irrespective of pathogen environment, figure 3), suggesting a protective and also a nutritional effect of the symbiont in this genetic background, similarly to what we saw for the N2 wild-type background. Surprisingly, the significantly higher MYb11-colonization rate in the *dbl-1* mutant does not translate into a higher competitive fitness relative to N2 (figure 4*b*), indicating that the higher MYb11 colonization rate alone is not the most critical determinant of nematode fitness.

The results for the *phm-2* mutant confirm that high colonization rates with the protective symbiont MYb11 do not necessarily improve performance of *C. elegans* in a pathogen environment. The *phm-2* mutant has a defective grinder in its pharynx, which was shown to increase accumulation of living bacteria in the intestine [72,73]. We similarly observed a significant increase in colonization by MYb11 and a moderate although insignificant higher abundance of pathogenic

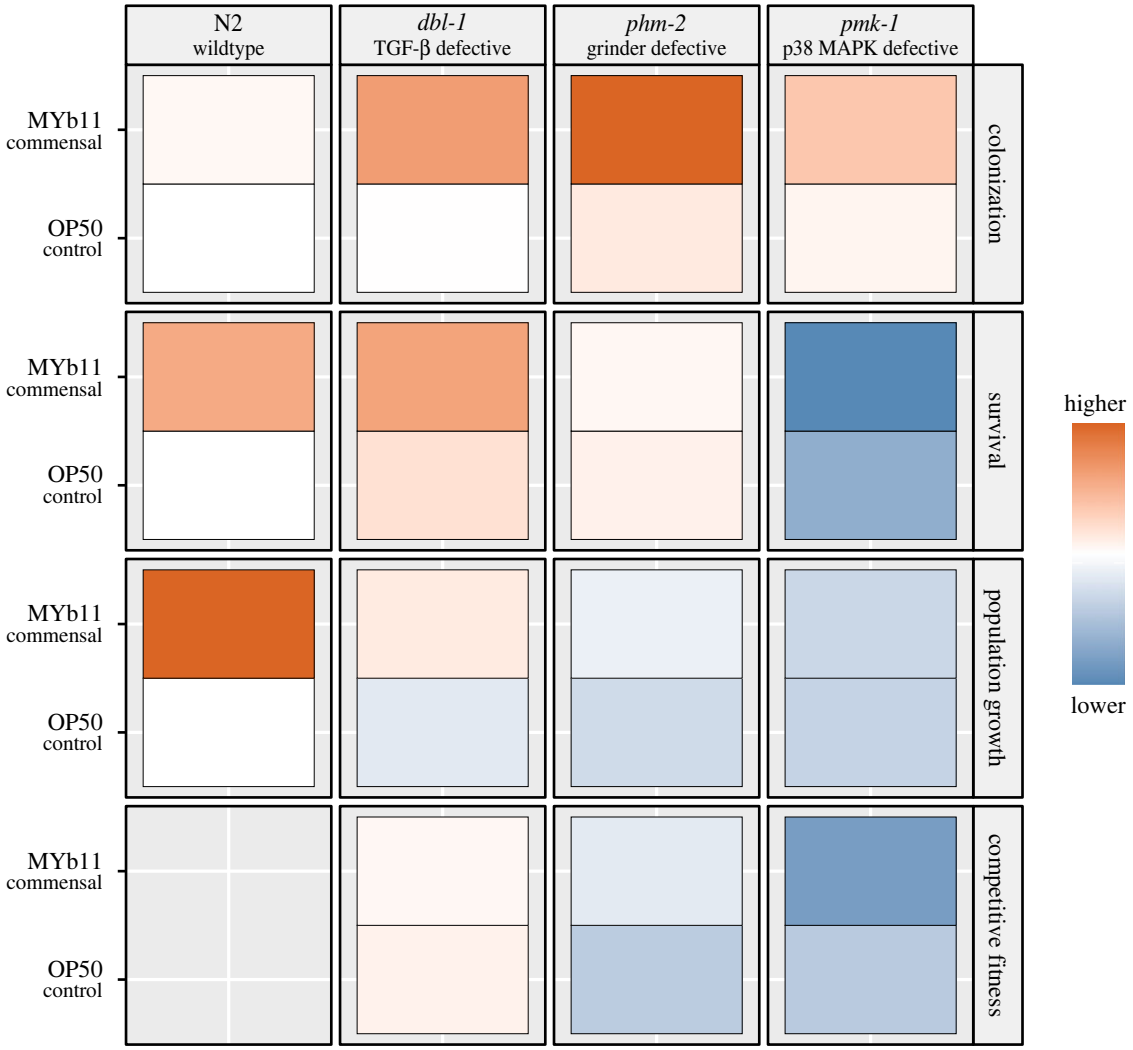

Figure 5. Overview of the main findings. For colonization, survival and population growth a heatmap was created showing the difference between the mean value per treatment (different *C. elegans* mutants combined with either protective *P. lurida* MYb11 or the standard laboratory food bacterium *E. coli* OP50) and the mean value obtained for the *C. elegans* wild-type N2 with the food bacterium OP50 as reference. Orange indicates higher values and blue lower values than the reference. Colonization and population growth data were square root transformed for illustration. For competitive fitness, the heatmap shows higher fitness (orange) or lower fitness (blue) compared to the wild-type either on MYb11 or OP50. For this overview, we only considered the results obtained upon infection with pathogenic *B. thuringiensis* Bt679.

Bt679 (figure 1). The increased MYb11 colonization did not lead to any change in survival in the presence of the pathogen (figure 2), but it resulted in increased population growth (figure 3) and also slightly (albeit insignificantly) increased competitive fitness (figure 4)—always in comparison to the Bt407 or *E. coli* OP50 control. Population growth and competitive fitness of the MYb11 colonized mutants with the pathogen are either lower or not significantly different from the wild-type N2 measured under the same conditions. Unexpectedly, the competitive fitness of the *phm-2* mutant under pathogen-free conditions is significantly lower compared to wild-type N2. Overall, these results suggest that the defective grinder mutant is generally not as fit as the wild-type, possibly because of less efficient processing of bacterial food. At the same time, it does not suffer significantly more from pathogen infection compared to N2, while the increased colonization with the protective microbe enhances only offspring production but not survival, thereby revealing a trait-specific effect of the protective microbe in this genotypic host background that differs from the more consistent MYb11-dependent effects in the *dbl-1* mutant background.

The most unexpected results were obtained for the *pmk-1* mutant. The *pmk-1* gene encodes the p38 MAPK and is thus a central component of the p38 MAPK signalling cascade, which is one of the main *C. elegans* immunity pathways involved in the defence against diverse pathogen taxa and types [44], including the *B. thuringiensis* strain Bt679 used here [43]. In detail, *B. thuringiensis* produces crystal pore-forming toxins that damage the epithelial membranes of their targets [43,74]. The p38 MAPK pathway plays an essential role in host defence against these toxins [43,75,76], as shown for the Bt toxins Cry5B and Cry21A [40]. Cry21Aa3, a subfamily of Cry21A, is expressed by Bt679 [43,74]. Disruption of the p38 MAPK pathway in *pmk-1* mutants may therefore lead to increased toxin concentrations and epithelial damage, which should cause a decrease in survival, population growth and competitiveness, as we observed in the current study (figures 2–4). Intriguingly, MYb11 colonization was higher in Bt679-infected *pmk-1* mutants, but this effect led to a significant reduction in survival and competitiveness upon pathogen infection. Thus, the protective MYb11 makes it worse for an immunocompromised host in the presence of the pathogen. A possible

explanation for this result is the increased damage caused by Bt679 infection in the immunocompromised host, which can promote the translocation of intestinal microbiota into the body cavity. There, the microbes may feed on damaged host tissue, thus enhancing bacterial proliferation and ultimately causing host death, as previously reported for insects infected with insecticidal *B. thuringiensis* [77,78]. MYb11 may thus exploit changes in the host environment to increase its own fitness. These findings support previous work showing that MYb11 need not always be beneficial, but that it has pathogenic potential depending on the context [51]. Moreover, the results highlight the importance of an intact immune response targeted at the infecting pathogen, as provided by the non-disrupted p38 MAPK pathway in the N2 wild-type, as a basis for an additional protective effect of the microbiota, including MYb11, then leading to the better performance of the MYb11-colonized N2 wild-type upon pathogen infection when compared to the corresponding treatments of the *pmk-1* mutant for all measured traits (figures 2–4). This result is generally consistent with the previous report for *C. elegans*, where expression of a host lysozyme disproportionately suppressed the pathogenic *S. aureus* resulting in enhanced protection by *E. faecalis* [39].

We were surprised to see that the observed population growth rates, measured for each host strain alone, do not directly translate into competitive fitness. More specifically, all mutants produced significantly lower population growth rates than the wild-type N2 under almost all of the tested conditions (figure 3). This could have been expected for disruption of the *dbl-1* and *phm-2* genes, which was previously reported in both cases to cause reduced offspring numbers [73,79]. However, the lower population growth rates observed here only led to lower mutant competitiveness in four cases, the *phm-2* mutant assayed under pathogen-free conditions and the *pmk-1* mutant under pathogen conditions (always in comparison to N2; figure 4). This was not the case for the other relevant cases, most notably for the *dbl-1* mutant, which did not differ significantly in competitiveness from N2 under all tested conditions (figure 4). These results highlight the importance of measuring fitness of a particular genotype not only when it is studied alone but also when in competition with other genotypes.

In summary, our study demonstrates that the host genotype critically determines the beneficial effects of a protective symbiont in the presence of a pathogen. In certain genomic contexts, the symbiont can provide protection, whereas in other genomic contexts it can further decrease survival and fitness, which we observed in mutants with a disrupted immune response towards the considered pathogen. Therefore, the particular characteristics of the triangular interaction between host, protective microbe and pathogen need to be considered for a full understanding of metaorganism fitness. The here described relationships have been inferred with a simplified model and, thus, they are likely even more complex under realistic conditions with a much more speciose and dynamic microbiota community.

Ethics. The study included work with the nematode *C. elegans*, which is not subject to any legal restrictions.

Data accessibility. All data generated or analysed during this study are included in this published article and its electronic supplementary material files [80].

Declaration of AI use. We have not used AI-assisted technologies in creating this article.

Authors' Contributions. H.G.-K.: formal analysis, investigation, methodology, visualization, writing—original draft, writing—review and editing; C.P.: formal analysis, investigation, methodology, supervision, writing—original draft, writing—review and editing; I.K.H.: investigation, methodology, writing—review and editing; H.S.: conceptualization, funding acquisition, supervision, writing—original draft, writing—review and editing.

All authors gave final approval for publication and agreed to be held accountable for the work performed therein.

Conflict of interest declaration. The authors declare no competing financial interests.

Funding. Funding for this project was provided by the German Science Foundation within the Collaborative Research Centre CRC 1182 on Origin and Function of Metaorganisms, projects A1.1 (H.S., C.P., I.K.H.) and the Max-Planck Society (fellowship to H.S.).

Acknowledgements. We thank the Schulenburg group for helpful feedback, and the Caenorhabditis Genetics Center (CGC), funded by the National Institutes of Health (NIH) Office of Research Infrastructure Programs (P40 OD010440), for providing the *C. elegans* strains and *E. coli* OP50. Illustrations for experimental designs were created using BioRender.com.

References

1. Lynch JB, Hsiao EY. 2019 Microbiomes as sources of emergent host phenotypes. *Science* **365**, 1405–1409. (doi:10.1126/science.aay0240)
2. Rosenberg E, Zilber-Rosenberg I. 2018 The hologenome concept of evolution after 10 years. *Microbiome* **6**, 78. (doi:10.1186/s40168-018-0457-9)
3. Mcfall-Ngai M *et al.* 2013 Animals in a bacterial world, a new imperative for the life sciences. *Proc. Natl Acad. Sci. USA* **110**, 3229–3236. (doi:10.1073/pnas.1218525110)
4. Bosch TCG, Mcfall-Ngai MJ. 2011 Metaorganisms as the new frontier. *Zoology* **114**, 185–190. (doi:10.1016/j.zool.2011.04.001)
5. Zilber-Rosenberg I, Rosenberg E. 2008 Role of microorganisms in the evolution of animals and plants: the hologenome theory of evolution. *FEMS Microbiol. Rev.* **32**, 723–735. (doi:10.1111/j.1574-6976.2008.00123.x)
6. Kolodny O, Schulenburg H. 2020 Microbiome-mediated plasticity directs host evolution along several distinct time scales. *Phil. Trans. R. Soc. B* **375**, 20190589. (doi:10.1098/rstb.2019.0589)
7. Bordenstein SR, Theis KR. 2015 Host biology in light of the microbiome: ten principles of holobionts and hologenomes. *PLoS Biol.* **13**, e1002226. (doi:10.1371/journal.pbio.1002226)
8. Henry LP, Bruijning M, Forsberg SKG, Ayroles JF. 2021 The microbiome extends host evolutionary potential. *Nat. Commun.* **12**, 5141. (doi:10.1038/s41467-021-25315-x)
9. Mclaren MR, Callahan BJ. 2020 Pathogen resistance may be the principal evolutionary advantage provided by the microbiome. *Phil. Trans. R. Soc. B* **375**, 20190592. (doi:10.1098/rstb.2019.0592)
10. Deriu E, Liu JZ, Pezeshki M, Edwards RA, Ochoa RJ, Contreras H, Libby SJ, Fang FC, Raffatellu M. 2013 Probiotic bacteria reduce *Salmonella* Typhimurium intestinal colonization by competing for iron. *Cell Host Microbe* **14**, 26–37. (doi:10.1016/j.chom.2013.06.007)
11. Kamada N, Kim YG, Sham HP, Vallance BA, Puente JL, Martens EC, Núñez G. 2012 Regulated virulence controls the ability of a pathogen to compete with the gut microbiota. *Science* **336**, 1325–1329. (doi:10.1126/science.1222195)
12. Jacobson A *et al.* 2018 A gut commensal-produced metabolite mediates colonization resistance to *Salmonella* infection. *Cell Host Microbe* **24**, 296–307. (doi:10.1016/j.chom.2018.07.002)

13. Corr SC, Li Y, Riedel Cu OPW, Hill C, Gahan Cg M. 2007 Bacteriocin production as a mechanism for the antiinfective activity of *Lactobacillus salivarius* UCC118. *Proc. Natl Acad. Sci. USA* **104**, 7617–7621. (doi:10.1073/pnas.0700440104)
14. Thiemann S *et al.* 2017 Enhancement of IFNγ production by distinct commensals ameliorates *Salmonella*-induced disease. *Cell Host Microbe* **21**, 682–694. (doi:10.1016/j.chom.2017.05.005)
15. Clarke TB, Davis KM, Lysenko ES, Zhou AY, Yu Y, Weiser JN. 2010 Recognition of peptidoglycan from the microbiota by Nod1 enhances systemic innate immunity. *Nat. Med.* **16**, 228–231. (doi:10.1038/nm.2087)
16. Sequeira RP, Mcdonald JAK, Marchesi JR, Clarke TB. 2020 Commensal bacteroidetes protect against *Klebsiella pneumoniae* colonization and transmission through IL-36 signalling. *Nat. Microbiol.* **5**, 304–313. (doi:10.1038/s41564-019-0640-1)
17. Desai MS *et al.* 2016 A dietary fiber-deprived gut microbiota degrades the colonic mucus barrier and enhances pathogen susceptibility. *Cell* **167**, 1339–1353. (doi:10.1016/j.cell.2016.10.043)
18. Taur Y, Pamer EG. 2013 The intestinal microbiota and susceptibility to infection in immunocompromised patients. *Curr. Opin Infect. Dis.* **26**, 332–337. (doi:10.1097/QCO.0b013e3283630dd3)
19. Seelbinder B *et al.* 2020 Antibiotics create a shift from mutualism to competition in human gut communities with a longer-lasting impact on fungi than bacteria. *Microbiome* **8**, 133. (doi:10.1186/s40168-020-00899-6)
20. D'enfert C *et al.* 2021 The impact of the fungus–host–microbiota interplay upon *Candida albicans* infections: Current knowledge and new perspectives. *FEMS Microbiol. Rev.* **45**, 1–55. (doi:10.1093/femsre/fuaa060)
21. Stevens EJ, Bates KA, King KC. 2021 Host microbiota can facilitate pathogen infection. *PLoS Pathog.* **17**, e1009514. (doi:10.1371/journal.ppat.1009514)
22. Tovaglieri A *et al.* 2019 Species-specific enhancement of enterohemorrhagic *E. coli* pathogenesis mediated by microbiome metabolites. *Microbiome* **7**, 43. (doi:10.1186/s40168-019-0650-5)
23. Stecher BÃ¤ *et al.* 2007 *Salmonella enterica* serovar Typhimurium exploits inflammation to compete with the intestinal microbiota. *PLoS Biol.* **5**, 2177–2189. (doi:10.1371/journal.pbio.0050244)
24. Pickard JM, Zeng MY, Caruso R, Núñez G. 2017 Gut microbiota: role in pathogen colonization, immune responses, and inflammatory disease. *Immunol. Rev.* **279**, 70–89. (doi:10.1111/imr.12567)
25. Wei G, Lai Y, Wang G, Chen H, Li F, Wang S. 2017 Insect pathogenic fungus interacts with the gut microbiota to accelerate mosquito mortality. *Proc. Natl Acad. Sci. USA* **114**, 5994–5999. (doi:10.1073/pnas.1703546114)
26. Winglee K, Eloe-Fadrosh E, Gupta S, Guo H, Fraser C, Bishai W. 2014 Aerosol *Mycobacterium tuberculosis* infection causes rapid loss of diversity in gut microbiota. *PLoS ONE* **9**, e97048. (doi:10.1371/journal.pone.0097048)
27. Bosch TCG. 2014 Rethinking the role of immunity: lessons from *Hydra*. *Trends Immunol.* **35**, 495–502. (doi:10.1016/j.it.2014.07.008)
28. Zhang F *et al.* 2021 Natural genetic variation drives microbiome selection in the *Caenorhabditis elegans* gut. *Curr. Biol.* **31**, 2603–2618. (doi:10.1016/j.cub.2021.04.046)
29. Berg M, Monnin D, Cho J, Nelson L, Crits-Christoph A, Shapira M. 2019 TGFβ/BMP immune signaling affects abundance and function of *C. elegans* gut commensals. *Nat. Commun.* **10**, 604. (doi:10.1038/s41467-019-08379-8)
30. Marra A, Hanson MA, Kondo S, Erkosar B, Lemaitre B. 2021 *Drosophila* antimicrobial peptides and lysozymes regulate gut microbiota composition and abundance. *mBio* **12**, e00824-21. (doi:10.1128/mBio.00824-21)
31. Fink C, Hoffmann J, Knop M, Li Y, Isermann K, Roeder T. 2016 Intestinal FoxO signaling is required to survive oral infection in *Drosophila*. *Mucosal Immunol.* **9**, 927–936. (doi:10.1038/mi.2015.112)
32. Nyholm SV, Mcfall-Ngai MJ. 2021 A lasting symbiosis: how the Hawaiian bobtail squid finds and keeps its bioluminescent bacterial partner. *Nat. Rev. Microbiol.* **19**, 666–679. (doi:10.1038/s41579-021-00567-y)
33. Ansaldo E, Farley TK, Belkaid Y. 2021 Control of immunity by the microbiota. *Annu. Rev. Immunol.* **39**, 449–479. (doi:10.1146/annurev-immunol-093019-112348)
34. Rooks MG, Garrett WS. 2016 Gut microbiota, metabolites and host immunity. *Nat. Rev. Immunol.* **16**, 341–352. (doi:10.1038/nri.2016.42)
35. Armitage SA, Genersch E, Mcmahon DP, Rafaluk-Mohr C, Rolff J. 2022 Tripartite interactions: how immunity, microbiota and pathogens interact and affect pathogen virulence evolution. *Curr. Opin. Insect. Sci.* **50**, 100871. (doi:10.1016/j.cois.2021.12.011)
36. Gerardo NM, Hoang KL, Stoy KS. 2020 Evolution of animal immunity in the light of beneficial symbioses. *Phil. Trans. R. Soc. B* **375**, 20190601. (doi:10.1098/rstb.2019.0601)
37. King KC *et al.* 2016 Rapid evolution of microbe-mediated protection against pathogens in a worm host. *ISME J.* **10**, 1915–1924. (doi:10.1038/ismej.2015.259)
38. Rafaluk-Mohr C, Ashby B, Dahan DA, King KC. 2018 Mutual fitness benefits arise during coevolution in a nematode-defensive microbe model. *Evol. Lett.* **2**, 246–256. (doi:10.1002/evl3.58)
39. Ford SA, Drew GC, King KC. 2022 Immune-mediated competition benefits protective microbes over pathogens in a novel host species. *Heredity* **129**, 327–335. (doi:10.1038/s41437-022-00569-3)
40. Huffman DL, Abrami L, Sasik R, Corbeil J, Van Der Goot FG, Aroian RV. 2004 Mitogen-activated protein kinase pathways defend against bacterial pore-forming toxins. *Proc. Natl Acad. Sci. USA* **101**, 10 995–11 000. (doi:10.1073/pnas.0404073101)
41. Hasshoff M, Höhnisch C, Tonn D, Hasert B, Schulenburg H. 2007 The role of *Caenorhabditis elegans* insulin-like signaling in the behavioral avoidance of pathogenic *Bacillus thuringiensis*. *FASEB J.* **21**, 1801–1812. (doi:10.1096/fj.06-6551com)
42. Wang J, Nakad R, Schulenburg H. 2012 Activation of the *Caenorhabditis elegans* FOXO family transcription factor DAF-16 by pathogenic *Bacillus thuringiensis*. *Dev. Comp. Immunol.* **37**, 193–201. (doi:10.1016/j.dci.2011.08.016)
43. Zárate-Potes A *et al.* 2020 The *C. elegans* GATA transcription factor *elt-2* mediates distinct transcriptional responses and opposite infection outcomes towards different *Bacillus thuringiensis* strains. *PLoS Pathog.* **16**, e1008826. (doi:10.1371/journal.ppat.1008826)
44. Martineau CN, Kirienko NV, Pujol N. 2021 Innate immunity in *C. elegans*. *Curr. Top. Dev. Biol.* **144**, 309–351. (doi:10.1016/bs.ctdb.2020.12.007)
45. Zhang F, Berg M, Dierking K, Félix MA, Shapira M, Samuel BS, Schulenburg H. 2017 *Caenorhabditis elegans* as a model for microbiome research. *Front. Microbiol.* **8**, 485. (doi:10.3389/fmicb.2017.00485)
46. Petersen C, Hamerich IK, Adair KL, Griem-Krey H, Torres Oliva M, Hoeppner MP, Bohannan BJM, Schulenburg H. 2023 Host and microbiome jointly contribute to environmental adaptation. *ISME J.* **17**, 1953–1965. (doi:10.1038/s41396-023-01507-9)
47. Obeng N *et al.* 2023 Bacterial c-di-GMP has a key role in establishing host–microbe symbiosis. *Nat. Microbiol.* **8**, 1809–1819. (doi:10.1038/s41564-023-01468-x)
48. Dirksen P *et al.* 2016 The native microbiome of the nematode *Caenorhabditis elegans*: Gateway to a new host-microbiome model. *BMC Biol.* **14**, 38. (doi:10.1186/s12915-016-0258-1)
49. Johnke J, Dirksen P, Schulenburg H. 2020 Community assembly of the native *C. elegans* microbiome is influenced by time, substrate and individual bacterial taxa. *Environ. Microbiol.* **22**, 1265–1279. (doi:10.1111/1462-2920.14932)
50. Kissoyan KAB, Drechsler M, Stange EL, Zimmermann J, Kaleta C, Bode HB, Dierking K. 2019 Natural *C. elegans* microbiota protects against infection via production of a cyclic lipopeptide of the viscosin group. *Curr. Biol.* **29**, 1030–1037. (doi:10.1016/j.cub.2019.01.050)
51. Kissoyan KAB, Peters L, Giez C, Michels J, Pees B, Hamerich IK, Schulenburg H, Dierking K. 2022 Exploring effects of *C. elegans* protective natural microbiota on host physiology. *Front. Cell Infect. Microbiol.* **12**, 775728. (doi:10.3389/fcimb.2022.775728)
52. Taylor M, Vega NM. 2021 Host immunity alters community ecology and stability of the microbiome in a *Caenorhabditis elegans* model. *mSystems* **6**, e00608–20. (doi:10.1128/msystems.00608-20)
53. Ortiz A, Vega NM, Ratzke C, Gore J. 2021 Interspecies bacterial competition regulates community assembly in the *C. elegans* intestine. *ISME J.* **15**, 2131–2145. (doi:10.1038/s41396-021-00910-4)
54. Stiernagle T. 2006 Maintenance of *C. elegans*. *WormBook*, 1–11. (doi:10.1895/wormbook.1.101.1)

55. Borgonie G, Van Driessche R, Leyns F, Arnaut G, De Waele D, Coomans A. 1995 Germination of *Bacillus thuringiensis* spores in bacteriophagous nematodes (Nematoda: Rhabditida). *J. Invertebr. Pathol.* **65**, 61–67. (doi:10.1006/jipa.1995.1008)
56. Dirksen P *et al.* 2020 CeMbio - the *Caenorhabditis elegans* microbiome resource. *G3: Genes, Genomes, Genetics* **10**, 3025–3039. (doi:10.1534/g3.120.401309)
57. Pees B *et al.* 2021 Effector and regulator: diverse functions of *C. elegans* C-type lectin-like domain proteins. *PLoS Pathog.* **17**, e1009454. (doi:10.1371/journal.ppat.1009454)
58. Petersen C, Saebelfeld M, Barbosa C, Pees B, Hermann RJ, Schalkowski R, Strathmann EA, Dirksen P, Schulenburg H. 2015 Ten years of life in compost: temporal and spatial variation of North German *Caenorhabditis elegans* populations. *Ecol. Evol.* **5**, 3250–3263. (doi:10.1002/ece3.1605)
59. Fay DS, Fluet A, Johnson CJ, Link CD. 1998 *In vivo* aggregation of β-amyloid peptide variants. *J. Neurochem.* **71**, 1616–1625. (doi:10.1046/j.1471-4159.1998.71041616.x)
60. R Core Team. 2021 *R: A language and environment for statistical computing*. Vienna, Austria: R foundation for statistical Computing.
61. Wickham H. 2016 *ggplot2: Elegant graphics for data analysis*. Cham, Switzerland: Springer. (doi:10.1007/978-3-319-24277-4)
62. Shapiro SS, Wilk MB. 1965 An analysis of variance test for normality (complete samples). *Biometrika* **52**, 591–611. (doi:10.2307/2333709)
63. Snedecor GW, Cochran WG. 1989 *Statistical methods*, 8th edn. Ames, IA: Iowa State University Press.
64. Nelder JA, Wedderburn RWM. 1972 Generalized linear models. *J. R. Stat. Soc. Ser. A* **135**, 370–384. (doi:10.2307/2344614)
65. Dunn OJ. 1961 Multiple comparisons among means. *J. Am. Stat. Assoc.* **56**, 52–64. (doi:10.1080/01621459.1961.10482090)
66. Wilcoxon F. 1945 Individual comparisons by ranking methods. *Biometrics Bull.* **1**, 80–83. (doi:10.2307/3001968)
67. Student. 1908 The probable error of a mean. *Biometrika* **6**, 1–25. (doi:10.2307/2331554)
68. Benjamini Y, Hochberg Y. 1995 Controlling the false discovery rate: a practical and powerful approach to multiple testing. *J. R. Stat. Soc. B* **57**, 289–300. (doi:10.1111/j.2517-6161.1995.tb02031.x)
69. Otarigho B, Aballay A. 2020 Cholesterol regulates innate immunity via nuclear hormone receptor NHR-8. *iScience* **23**, 101068. (doi:10.1016/j.isci.2020.101068)
70. Zugasti O, Ewbank JJ. 2009 Neuroimmune regulation of antimicrobial peptide expression by a noncanonical TGF-β signaling pathway in *Caenorhabditis elegans* epidermis. *Nat. Immunol.* **10**, 249–256. (doi:10.1038/ni.1700)
71. Mallo GV, Lé Opold Kurz C, Couillault C, Pujol N, Granjeaud S, Kohara Y, Ewbank JJ. 2002 Inducible antibacterial defense system in *C. elegans*. *Curr. Biol.* **12**, 1209–1214. (doi:10.1016/s0960-9822(02)00928-4)
72. Portal-Celhay C, Bradley ER, Blaser MJ. 2012 Control of intestinal bacterial proliferation in regulation of lifespan in *Caenorhabditis elegans*. *BMC Microbiol.* **12**, 49. (doi:10.1186/1471-2180-12-49)
73. Kumar S, Egan BM, Kocsisova Z, Schneider DL, Murphy JT, Diwan A, Kornfeld K. 2019 Lifespan extension in *C. elegans* caused by bacterial colonization of the intestine and subsequent activation of an innate immune response. *Dev. Cell* **49**, 100–117. (doi:10.1016/j.devcel.2019.03.010)
74. Masri L *et al.* 2015 Host-pathogen coevolution: the selective advantage of *Bacillus thuringiensis* virulence and its Cry toxin genes. *PLoS Biol.* **13**, e1002169. (doi:10.1371/journal.pbio.1002169)
75. Bischof LJ, Kao CY, Los FCO, Gonzalez MR, Shen Z, Briggs SP, Van Der Goot FG, Aroian RV. 2008 Activation of the unfolded protein response is required for defenses against bacterial pore-forming toxin *in vivo*. *PLoS Pathog.* **4**, e1000176. (doi:10.1371/journal.ppat.1000176)
76. Porta H, Cancino-Rodezno A, Soberón M, Bravo A. 2011 Role of MAPK p38 in the cellular responses to pore-forming toxins. *Peptides* **32**, 601–606. (doi:10.1016/j.peptides.2010.06.012)
77. Caccia S *et al.* 2016 Midgut microbiota and host immunocompetence underlie *Bacillus thuringiensis* killing mechanism. *Proc. Natl Acad. Sci. USA* **113**, 9486–9491. (doi:10.1073/pnas.1521741113)
78. Broderick NA, Raffa KF, Handelsman J. 2006 Midgut bacteria required for *Bacillus thuringiensis* insecticidal activity. *Proc. Natl Acad. Sci. USA* **103**, 15 196–15 199. (doi:10.1073/pnas.0604865103)
79. Luo S, Shaw WM, Ashraf J, Murphy CT. 2009 TGF-ß Sma/Mab signaling mutations uncouple reproductive aging from somatic aging. *PLoS Genet.* **5**, e1000789. (doi:10.1371/journal.pgen.1000789)
80. Griem-Krey H, Petersen C, Hamerich IK, Schulenburg H. 2023 The intricate triangular interaction between protective microbe, pathogen and host determines fitness of the metaorganism. Figshare. (doi:10.6084/m9.figshare.c.6935806)